scientific reports

Check for updates

OPEN

A single dose of glycogen phosphorylase inhibitor improves cognitive functions of aged mice and affects the concentrations of metabolites in the brain

Natalia Pudełko-Malik[1,4], Dominika Drulis-Fajdasz[2,4], Łukasz Pruss[1,3], Karolina Anna Mielko-Niziałek[1], Dariusz Rakus[2], Agnieszka Gizak[2]✉ & Piotr Młynarz[1]✉

Inhibition of glycogen phosphorylase (Pyg) – a regulatory enzyme of glycogen phosphorolysis – influences memory formation in rodents. We have previously shown that 2-week intraperitoneal administration of a Pyg inhibitor BAY U6751 stimulated the "rejuvenation" of the hippocampal proteome and dendritic spines morphology and improved cognitive skills of old mice. Given the tedious nature of daily intraperitoneal drug administration, in this study we investigated whether a single dose of BAY U6751 could induce enduring behavioral effects. Obtained results support the efficacy of such treatment in significantly improving the cognitive performance of 20-22-month-old mice. Metabolomic analysis of alterations observed in the hippocampus, cerebellum, and cortex reveal that the inhibition of glycogen phosphorolysis impacts not only glucose metabolism but also various other metabolic processes.

Keywords Brain aging, Memory formation, Hippocampus, Glycogen phosphorylase (pyg), Behavioral tests, Metabolomics

Glycogen phosphorylase (Pyg) serves as the pivotal regulatory enzyme governing glycogen phosphorolysis. This enzymatic activity release α-D-glucose 1-phosphate, which is then used as a substrate in glycolysis to meet high energy demands. The activity of glycogen phosphorylase is tightly regulated through both allosteric mechanisms by AMP, ATP, ADP, and glucose-6-phosphate, and covalent modification (phosphorylation actives glycogen phosphorylase). The inhibitory modulation of Pyg has been demonstrated to impede the establishment of memory in young chickens and mice[1,2]. Additionally, this inhibition impedes the induction of Long-Term Potentiation (LTP), a cellular and molecular mechanism of memory formation, both in vivo and within hippocampal slices isolated from juvenile rodents[3,4]. The observed impairment in neuronal plasticity resulting from Pyg inhibition is concomitant with a diminished transfer of glycogen-derived lactate from astrocytes to neurons. This phenomenon, recognized as the Astrocyte-Neuronal Lactate Shuttle (ANLS), has been elucidated as a critical process in facilitating neuronal energy metabolism[5].

In contrast to young animals, the inhibition of glycogen degradation in hippocampal sections isolated from aged rodents has been observed to enhance the formation of Long-Term Potentiation (LTP) and exert an influence on the maturation of dendritic spines[4]. Furthermore, a prolonged 2-week treatment of aged mice with the Pyg inhibitor BAY U6751 (BAY) has demonstrated not only the capacity to rescue deficits in memory formation associated with aging but also to "rejuvenate" the hippocampal proteome[2].

The precise mechanisms governing this disparate response to Pyg inhibition remain inadequately understood; however, they may be linked to distinct organization of the hippocampal formation in young and aged animals[6], as well as age-related alterations in the expression of hippocampal proteins[7], and NAD^+/NADH metabolism[8]. These outcomes underscore the distinct role of astrocyte-derived lactate in neuronal plasticity between young and

[1]Department of Biochemistry, Molecular Biology and Biotechnology, Faculty of Chemistry, Wroclaw University of Science and Technology, Wybrzeże Wyspiańskiego 27, Wroclaw 50-370, Poland. [2]Department of Molecular Physiology and Neurobiology, University of Wroclaw, Sienkiewicza 21, Wroclaw 50- 335, Poland. [3]Ardigen, Kraków 30-394, Poland. [4]Natalia Pudełko-Malik and Dominika Drulis-Fajdasz contributed equally to this work. ✉email: agnieszka.gizak@uwr.edu.pl; piotr.mlynarz@pwr.edu.pl

old animals. Additionally, they reveal that in aged animals, the immediate impact of Pyg inhibition manifests as memory enhancement resulting from Astrocyte-Neuronal Lactate Shuttle (ANLS) disruption. In turn, sustained (2-week) blockade of the ANLS leads to a restoration of cognitive performance to levels observed in young animals, attributable to the rejuvenation of the hippocampal proteome and dendritic spines morphology[2]. These findings prompted an investigation into whether a single dose of the inhibitor is sufficient to induce a lasting improvement in the cognitive abilities of the animals.

Metabolomics approach is particularly advantageous in studying aging, where traditional genomic and proteomics methods have limitations. While these methods provide valuable information about age-related changes in gene and protein expression, they often miss the dynamic and complex metabolic shifts that occur during aging[9,10]. Metabolomics, by offering a direct and comprehensive analysis of low molecular weight metabolites (<1500 Da), especially when applied to global tissue analysis, can overcome these limitations by providing detailed view of tissues activity across a broad spectrum of metabolites, including those that are low-abundant and labile[11,12]. Application of global metabolomic analysis could significantly improve our understanding of the molecular foundations of brain aging by providing direct an imperial monitoring of metabolic pathways.

In our study we used Nuclear Magnetic Spectroscopy (NMR) technique, with demonstrates excellent potential in the context of studying neuronal tissue metabolites[13–15]. NMR spectroscopy provides both qualitative and quantitative information about around 10^2 small molecules in biological material, without needing to focus on specific biochemical pathways, which allows for a broad and unbiased analysis[11]. Additionally, NMR spectroscopy is known for its high reproducibility, non-invasiveness, and overall high quality[16]. A particularly advantageous feature is the simplicity of sample preparation, which typically involves a single-step extraction using aqueous solvents. This contrasts with methods like GC-MS or LC-MS, which often require additional steps such as derivatization. This analytical approach allows for multiple uses of the same sample, which is crucial when dealing with unique biological materials[17]. Additionally, it provides more reliable data by reducing variability within the repeated sample. This is especially important for biofluids and tissue extracts, as it accurately reflects the metabolic state of the living organism at a specific point in time.

In this study, we present several lines of evidence supporting the efficacy of a single intraperitoneal administration of BAY in significantly enhancing the cognitive performance of 20-22-month-old mice, as assessed through the Novel Object Location (NOL) and 2-Novel Object Recognition (NOR) tests. To elucidate the metabolic alterations induced by a single dose of the Pyg inhibitor, we conducted an untargeted metabolomic analysis. The results reveal that a single administration of BAY influences the titers of several metabolites associated with diverse biochemical pathways – not only those directly related to glycogen degradation – across all examined brain formations, irrespective of age.

Results and discussion

Behavioral studies

Results of our previous experiments[2], revealed the administration of a single daily dose of the glycogen phosphorylase inhibitor BAY U6751 (BAY) over 2 weeks led to a significant improvement in learning and object recognition in old mice, as tested using the 2-Novel Object Recognition and Novel Object Location tests. Conversely, young mice exhibited an opposite effect in response to BAY. Given the tedious nature of daily intraperitoneal drug administration, we sought to investigate whether a single dose of BAY could induce enduring behavioral effects.

The Novel Object Location (NOL) test was developed to assess spatial memory in rodents (see Materials and Methods, section Behavioral tests). In summary, the tested animal was placed in a box containing two identical objects for 10 min. Following short break, the animal was reintroduced to the same objects, but the position of one of the them has been altered. Healthy rodents with intact memory tend to spend more time exploring the object in the new location (see Materials and Methods, section Behavioral tests).

The Novel Object Recognition (NOR) test assesses the interactions of the multi-mode brain system in cognition, primarily associated with cortical and hippocampal functions[18]. In this test, following a learning episode of 10 min., one of two objects in a box was replaced with a new one, while the locations of the objects remain unchanged (Fig. 1a).

In the current experiment, the NOL and NOR tests were conducted on Day 0, one by one, following a week-long period of handling the mice. After an additional week, young, and aged mice received a single injection of BAY (see Materials and Methods, section Behavioral tests). 4.5 h post-injection, they underwent the NOL and NOR tests again (day "One Dose of BAY", Fig. 1a). The control groups were injected with a single dose of saline and then subjected to the same tests.

The effect of BAY U6751 on the NOL test-measured memory

Spatial memory is a complex cognitive ability crucial for survival, primarily associated with the hippocampus[19]. It is widely acknowledged that aging is linked to the impairment of various cognitive functions, particularly affecting navigation abilities[20]. Data obtained from the NOL test (see Materials and Methods, section Behavioral tests) conducted on the Day 0 (i.e., before the BAY administration) revealed expected disruption in spatial memory for old mice, in which no differences were found in the exploration time of constants vs. moved object ($p=0.96$) (Fig. 1c). At the same conditions, young mice properly explored the moved object significantly longer than the constant one ($p=0.003$) (Fig. 1b). Such analogical age-related differences in memory ability formation in the NOL test were also observed at day "One Dose of BAY"; for control groups i.e. following intraperitoneal saline administration. Young control mice spent significantly more time exploring the object placed in the new location (Y-CTR, $p=0.05$) (Fig. 1e). And again, there was no significant difference in the time spent exploring

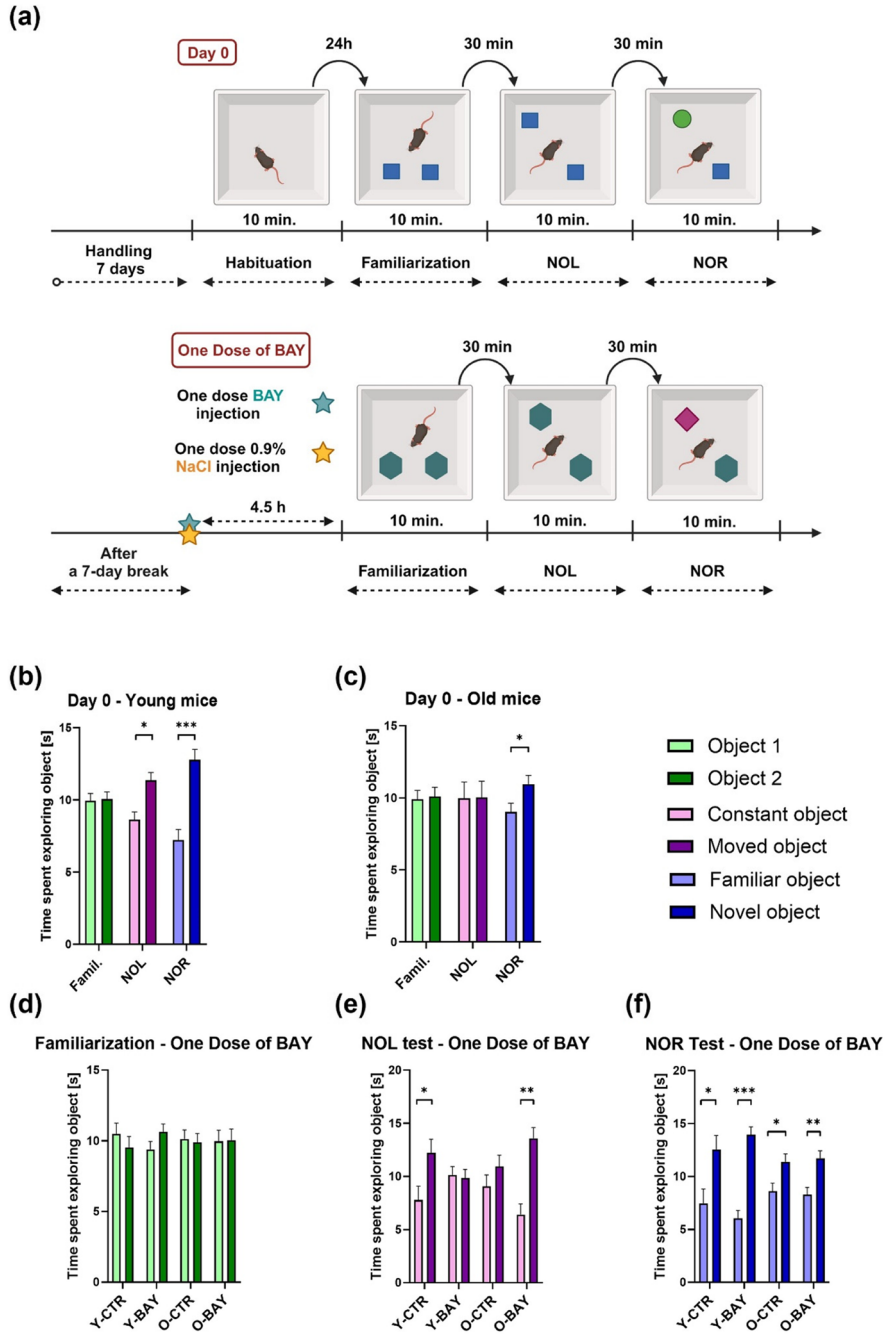

Figure 1. Inhibition of glycogen phosphorylase stimulates memory formation of 20-22-month-old mice. (**a**) Schematic representation of the behavioral experiment performed during "Day 0" and after a single dose of BAY U6751 administration ("One Dose of BAY"), for more details, please see Materials and Methods, section Behavioral tests (**b**, **c**) objects exploration time during the familiarization session (Famil.) and the NOL and NOR test at Day 0 obtained for control young (**b**) and old mice (**c**), (**d**-**f**) objects exploration time during the familiarization session (**d**) and the NOL (**e**) and NOR test (**f**) after a single dose of BAY U6751. Analyzed groups: young control (Y-CTR), young BAY treated (Y-BAY), old control (O-CTR), and old BAY treated (O-BAY). Comparing the NOL test data for Day 0 (**b**, **c**) and for "One Dose of BAY" (**e**), we observed a significant increase in spatial orientation in O-BAY mice and significantly decreased spatial orientation in Y-BAY mice. In control groups, we observed preserved spatial orientation (Y-CTR and O-CTR). Comparing the NOR test data for Day 0 (**b**, **c**) and for "One Dose of BAY" (**f**), the novel object recognition ability was generally preserved in all groups. The number of subjects in each experimental group $n = 7–10$. Data are presented as mean ± SEM (Standard Error of the Mean). The statistically significant changes between groups are indicated ($^{*}p < 0.05$; $^{**}p < 0.01$; $^{***}p < 0.001$).

at the two presented objects for aged control mice (O-CTR, $p=0.24$) (Fig. 1e), which is consistent with existing literature data[21].

Interestingly, we observed divergent age-related effects in BAY treated mice groups. A single dose of BAY U6751 injection disrupted the formation of spatial memory in young mice ("One Dose of BAY" time point; Y-BAY, $p=0.82$) (Fig. 1e). In contrast, such treatment in aged animals resulted in a significant improvement of spatial memory ($p<0.001$) (Fig. 1e). Our results suggest that a single dose of the inhibitor is sufficient to induce changes lasting at least 5 h (roughly the duration of the NOL test), similar to those observed after two-week treatment with glycogen phosphorylase inhibitor[2]. We did not find any signs of side preferences in the object exploration during familiarization sessions respectively for young animals at Day 0 ($p=0.89$) (Fig. 1b), old animals at Day 0 ($p=0.82$) (Fig. 1c), and for all analyzed animal groups at the "One Dose of BAY" time point (Y-CTR $p=0.43$, Y-BAY $p=0.2$, O-CTR $p=0.8$, and O-BAY $p=0.93$) (Fig. 1d) (see Materials and Methods, section Behavioral tests).

The effect of BAY U6751 on the NOR test-measured memory

The NOR test enables the investigation of short-term memory, intermediate-term memory, and long-term memory[22]. It is crucial to note that in our behavioral paradigm with short intersession interval lasting only 30 min, NOR test results are primarily associated with the function of the cerebral cortex rather than the hippocampus[23].

In our Day 0 experiment, young animals explored the novel object almost twice as long as the familiar one ($p<0.001$) (Fig. 1b, see Materials and Methods, section Behavioral tests). Aged mice also spent more time exploring the new object, albeit with a smaller difference, approximately 20% ($p=0.041$, Fig. 1c). Following a single injection of saline or BAY (at day "One Dose of BAY"), a preserved novelty recognition ability was observed in all analyzed groups (Y-CTR $p=0.03$, Y-BAY $p<0.001$, O-CTR $p=0.027$, O-BAY $p=0.0048$) (Fig. 1f).

These findings replicate and complement our previous NOR data obtained after a two-week treatment of mice with BAY U6751, wherein the NOR test paradigm involved a long (6 h) post-training break, and measured long-term memory formation ability[2]. Results obtained for control groups in our previous and present experiments suggest that the aged animals displayed worse cognitive skills in the long-term[2] than in the short-term (Fig. 1c), memory formation in novelty recognition experiments. However, BAY-treatment improved their long-term memory[2].

In conclusion, our experiments demonstrated that a single injection of BAY significantly improved hippocampus-based memory formation in aged mice while impairing the ability to form memory in young animals, as measured by the NOL test. On the other hand, BAY treatment had essentially no effect on the cortical component of cognitive performance, as measured by the NOR test.

Metabolomic studies

NMR – based metabolomic profiling of different mice brain areas

Metabolomic profiling was carried out using hippocampal, cortical and cerebellar tissue isolated immediately after the behavioral tests ("One Dose of BAY" time point) from control and BAY treated young and aged animals (see Materials and Methods, section Sample preparation and NMR measurment). The metabolomic approach based on one-dimensional (1D) NMR spectra allowed the identification of 27 metabolites across all studied samples, which belonged to a board metabolomic pathways, and was presented in Fig. 2 (for details refer to Supplementary Table S1 and Fig. 7a).

We identified several metabolites involved directly or indirectly in neuronal transmission. Among them were: γ - aminobutyric acid (GABA), glutamate (Glu), glutamine (Gln), crucial for maintaining excitation/inhibition equilibrium and involved in the Glu/GABA-Gln cycle. *N*-acetylaspartate (NAA) is an indicator for adult-type neurons and axons, Taurine (Tan) is a key marker of astrocytic activity, aspartate (Asp) which can act as NMDA receptor agonist in the brain and is linked to cognitive disorders. Glycine (Gly) is a neurotransmitter involved both in glycinergic and in glutamatergic transmission. Myo-inositol (Myo) is associated with cognitive and mood disorders[24], and pyridoxine participates e.g., in sphingosine phosphate metabolism and reduction of inflammation. We also identified several metabolites related to energy metabolism: succinate (Suc) and fumarate (Fum), known as important intermediate products of TCA cycle; lactate (Lac), a final product of anaerobic glycolysis; alanine (Ala) associated with the Glu/GABA-Gln cycle; and important gluconeogenic amino acid, creatine (Cre) and phosphocreatine (PCr), which play a key role in cellular energy buffering and energy transport. Other metabolites involved in the turnover of purine nucleotides (PNC, purine nucleotides cycle) included inosine (Ino), ATP, IMP, AMP, ADP and NAD^+. Finally, we detected metabolites belonging to various lipid metabolism-related processes: *O*-phosphocholine (Chop) and choline (Cho), essential components of cellular membranes; carnitine (Car), an important transporter of long-chain fatty acids; and *O*-phosphoethanolamine (PEA). Among other identified molecules were ascorbate (AA), beyond its crucial role in defense against oxidative stress, is suggested to play a function as a modulator of neuronal metabolism in some studies[25], and acetate, an energy substrate for astrocytes, which is also crucial for acetylcholine production and recycling of GABA and glutamate[26].

Utilizing principal component analysis (PCA) biplots (see Materials and Methods, section Univariate processing and statistical data analysis), we observed a clear separation of cerebellum samples from hippocampal and cortical samples, additionally highlighting the metabolites that contributed most to group separation (Fig. 3a).

Conversely, the metabolomic patterns of hippocampal and cortical samples exhibited partial overlap. The negative correlation observed between samples from the cerebellum, hippocampus, and cortex reflected the distinct functions of these brain formations. While the cerebellum primarily contributes to the coordination

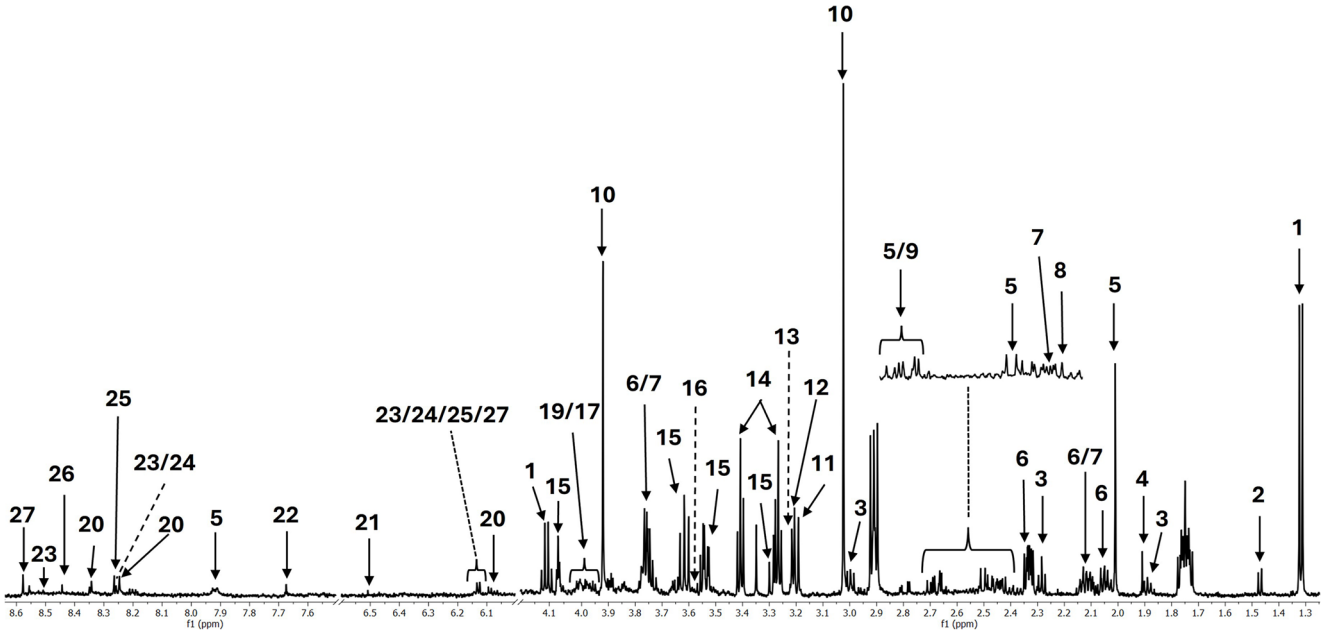

Figure 2. The representative high resolution ^{1}H NMRspectrum (600 MHz) of the extract of the hippocampus tissues taken from a young male mouse from the control group. *Peak 1* Lactate; *Peak 2* Alanine; *Peak 3* γ-Aminobutyric acid , *Peak 4* Acetate; *Peak 5 N-acetylaspartate*; *Peak 6* Glutamate; *Peak 7* Glutamine; *Peak 8* Succinate; *Peak 9* Aspartate; *Peak 10* Creatine; *Peak 11* Choline; *Peak 12 O* - phosphocholine; *Peak 13* Carnitine; *Peak 14* Taurine; *Peak 15 Myo*-inositol; *Peak 16* Glycine, *Peak 17 O- phosphoethanolamine, Peak 18* Ascorbate*, Peak 19* Phosphocreatine, *Peak 20* Inosine*, Peak 21* Fumarate*, Peak 22* Pyridoxine*, Peak 23* ADP, *Peak 24* ATP*, Peak 25* AMP, *Peak 26* NAD^{+}*, Peak 27* IMP.

and memory of voluntary movements[27], the hippocampus and cortex are predominantly responsible for more complex higher cognitive functions. Subsequently, we investigated whether the concentrations of identified metabolites were influenced by aging and/or glycogen phosphorylase inhibition. For that purpose, we compared their relative concentration across various groups: Y-CTR vs. Y-BAY, O-CTR vs. O-BAY, Y-CTR vs. O-CTR and Y-CTR vs. O-BAY, encompassing all examined brain formations (Fig. 3b-d).

Our analysis indicated that aging (comparison Y-CTR vs. O-CTR) led to a reduction in titers of approximately 33% of all detected metabolites in the hippocampus (Fig. 3b) and over 26% in the cerebellum (Fig. 3d), while only 4% of metabolites decreased their concentrations in the cortex (Fig. 3c). Notably, no metabolite concentrations increased with aging. These results underscored the heightened susceptibility of the hippocampal and cerebellar formations to age-related alterations compared to the cortex. BAY treatment of aged animals (comparison O-CTR vs. O-BAY) increased concentrations of 26% of metabolites in the hippocampus (Fig. 3b), ~12% in the cerebellum (Fig. 3d), and less than 4% in the cortex (Fig. 3c).

Strikingly, BAY treatment of aged mice induced a metabolic shift in the hippocampus toward juvenile-like characteristics (Y-CTR vs. O-BAY, Fig. 3b). In contrast, within the cortex and cerebellum of these mice, it led to an increase in the highest number of metabolites (Fig. 3c, d). Furthermore, the administration of BAY exerted a discernible impact on the metabolic profile of young animals (Y-CTR vs. Y-BAY, Fig. 3b-c). Motivated by these observations, we conducted a more comprehensive and detailed analysis of the metabolites across all examined brain formations.

The impact of the aging and BAY on hippocampal metabolome

The hippocampus is a pivotal brain structure for long-term episodic memory[28]. Metabolomic analysis of hippocampal tissue extracts derived from both young and aged mice, encompassing control and BAY-treated groups, revealed a multitude of qualitative alterations in the repertoire of metabolites implicated in energy production, signaling, and lipid metabolism (Fig. 4).

Among hippocampal metabolites, those exhibiting a decline in relative concentrations due to aging but experiencing a "rejuvenation" effect with BAY U6751 treatment (O-CTR vs. O-BAY) included alanine, PCr, GABA, aspartate, and PEA (Fig. 4). The titers of four other compounds – glutamate, ADP, taurine, and Chop – were significantly reduced by aging, but BAY U6751 treatment did not exert additional effects on them in aged mice (Fig. 4).Concentrations of glutamine and ascorbate did not decrease with age, yet BAY U6751 elevated glutamine level in both young and aged mice, and ascorbate in aged ones (Fig. 4).

Deregulation of neurotransmitters like GABA and glutamate signaling associated with aging has been previously documented[29,30]. GABA and glutamate, the primary inhibitory and excitatory neurotransmitters in the hippocampus, respectively, play a crucial role in cognitive functions[31]. Our findings, indicating a significant reduction in GABA and glutamate levels in the hippocampus of old mice, and an increase in GABA level after

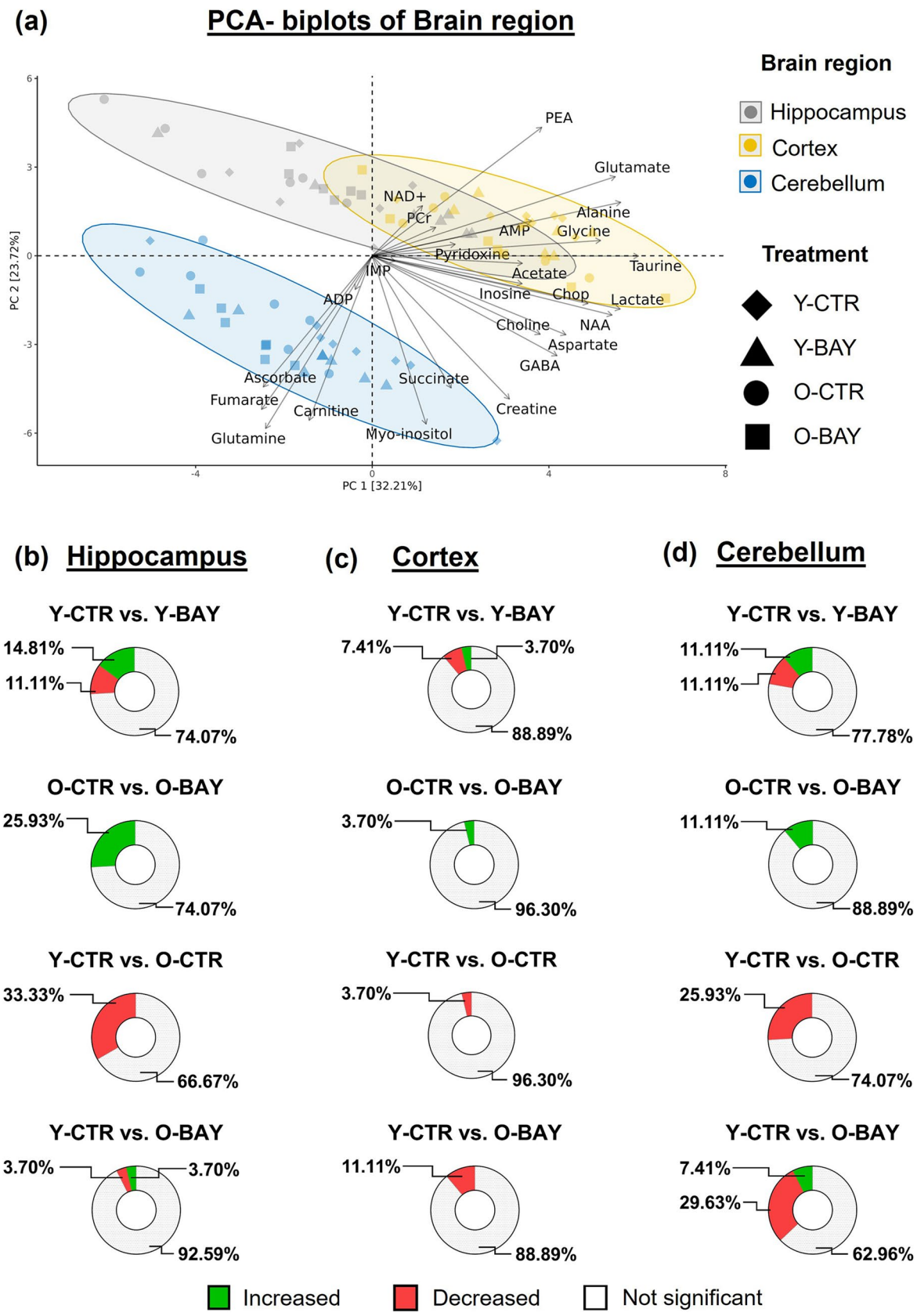
(a)
PCA- biplots of Brain region
Brain region
Hippocampus
Cortex
Cerebellum
Treatment
Y-CTR
Y-BAY
O-CTR
O-BAY
PC 2 [23.72%]
PC 1 [32.21%]
PEA
Glutamate
NAD+
PCr
Alanine
AMP
Glycine
Pyridoxine
Taurine
IMP
Acetate
Inosine
Chop
Lactate
ADP
Choline
NAA
Aspartate
GABA
Ascorbate
Succinate
Fumarate
Carnitine
Creatine
Glutamine
Myo-inositol
(b) Hippocampus
(c) Cortex
(d) Cerebellum
Y-CTR vs. Y-BAY
14.81%
11.11%
74.07%
7.41%
3.70%
88.89%
11.11%
11.11%
77.78%
O-CTR vs. O-BAY
25.93%
74.07%
3.70%
96.30%
11.11%
88.89%
Y-CTR vs. O-CTR
33.33%
66.67%
3.70%
96.30%
25.93%
74.07%
Y-CTR vs. O-BAY
3.70%
3.70%
92.59%
11.11%
88.89%
7.41%
29.63%
62.96%
Increased
Decreased
Not significant

◀**Figure 3**. Age-related metabolomic profiles and brain region-specific responses to BAY treatment. (**a**) Principal component analysis (PCA) biplots of principal component 1 and principal component 2 including loadings (identified metabolites were selected for quantification of relative integrals (see Table S1) for the hippocampus (gray ellipse), cortex (yellow ellipse), and cerebellum (blue ellipse) enclosing metabolic profiles of four animal groups: young controls (Y-CTR, diamonds); young BAY-treated (Y-BAY, triangles); old controls (O-CTR, circles); and old BAY-treated (O-BAY, squares). (**b**-**d**) Circular graphs reveal the relative integral contribution of all identified metabolites that were significantly or not significantly changed during aging and/or after BAY treatment, across analyzed brain subregions, in order: (**b**) hippocampus, (**c**) cortex, and (**d**) cerebellum. All identified metabolites in the study significantly increased or decreased are available in the supplementary materials (Table S2).

BAY treatment, align with the results of our behavioral studies, demonstrating that the aging-related decline in cognitive skills can be at least partially rescued by BAY administration (Fig. 1c vs. 1f). Moreover, the BAY induced increase of glutamine levels correlated with an increase in alanine, in old but not in young animals (Fig. 4). Alanine participates in the glutamate/glutamine cycle, which occurs between neurons and astrocytes. In this cycle, alanine acts as a nitrogen donor, providing ammonia for glutamine synthesis[32–34].

The significant decrease in Chop and PEA observed in the aged hippocampus (Fig. 4) indicates alterations in lipid metabolism. These metabolites are involved in phospholipid turnover and serve as precursors for biosynthesis of phosphatidylcholine[35], an essential lipid compound in cellular membranes[36]. The decreased titer of PEA correlates with neuronal loss and is commonly observed in Alzheimer's and Huntington's diseases[37–39].

On the other hand, PCr, increased in the aged hippocampi by BAY treatment, functions as an energy reservoir, maintaining a high cytosolic ATP/ADP ratio, and is highly abundant in striated muscle fibers, heart, and nerve cells. PCr plays a protective role in response to anoxic damage in hippocampal slices[40]. Notably, the absence of creatine phosphokinase, the enzyme facilitating phosphate group transfer to and from PCr[40], directly affects synapse efficiency in the hippocampal formation and influences habituation and spatial learning[41].

Interestingly, we observed divergent effects of BAY on young compared to old animals. In contrast to O-BAY animals, in the Y-BAY mice, a decrease in the levels of PEA and PCr was detected (Fig. 4). Furthermore, concentrations of five other metabolites were changed by the BAY treatment solely in young animals (reduction of IMP; increase of inosine, AMP, glutamine, and choline; Fig. 4). The opposite influence of BAY on young and old hippocampus metabolite profiles (Y-BAY vs. O-BAY) is consistent with the divergent behavioral hippocampus-dependent results of the young vs. old BAY-injected mice in the NOL test (Fig. 1e).

The impact of the aging and BAY on the cortex metabolome

Among all the examined regions, the cerebral cortex displayed the fewest significant changes in metabolite fingerprints induced by aging and/or BAY administration (Fig. 5).

Among all metabolites used for statistical analysis only 7 of them were affected by aging or BAY treatment. Fumarate was the sole metabolite reduced by aging. Although fumarate is an intermediate of the Krebs cycle, it has also been hypothesized to participate in antioxidative stress responses and protection against neurodegeneration[42]. BAY treatment increased the level of fumarate in the cortex of aged animals. However, due to high variations between individual mice in response to the inhibitor, the change was not statistically significant.

The cortex metabolome stayed mostly unchanged in old mice after the injection of BAY: only AMP showed a significant increase in titer (O-CTR vs. O-BAY; Fig. 5). More changes, although not as many as in the other structures, in cortex metabolome were detected in young BAY-treated mice. ADP and acetate titers were reduced by BAY while GABA showed increase after the glycogen breakdown inhibition (Fig. 5).

The observed cortex metabolome fingerprint stability is in line with the results of the cortex-dependent behavioral test (NOR), where the ability of mice to recognize the object novelty was preserved irrespective of aging or the BAY inhibitor presence (Fig. 1f).

The impact of aging and BAY on the cerebellum metabolome

The aging process significantly impacted the metabolic profile of the cerebellum. Our analysis revealed alterations across all the examined metabolite groups, particularly in signaling pathways where glutamate and glycine exhibited significant reductions in titers. Additionally, lipid metabolism displayed changes in the relative concentration of choline and Chop. Moreover, alterations were observed in energy metabolism, with metabolites such as succinate, inosine and AMP showing decreased concentrations. We observed also a decrease in ascorbate relative concentration (Fig. 6).

In contrast to the hippocampus, BAY administration only rescued the aging-associated decrease in succinate and ascorbate titers (Fig. 6). Overall, the effects of the inhibitor were more pronounced in the young cerebellum, significantly impacting the levels of IMP, ADP, glycine, pyridoxine, choline, and carnitine.

These observed alterations in metabolic patterns are consistent with the existing literature, which suggests that changes in the functional properties of the cerebellum due to aging are not attributable to large-scale cell loss but rather to a focused and regulated molecular process[43].

The variability in age-related changes in the cerebellum metabolome was partially reflected in mice behavior. Our previous data from the cerebellum-dependent RotaRod tests[2], differentiated between groups of young and old mice, but there were no effects of BAY treatment. This supports the idea that the cerebellum differs in synaptic plasticity mechanisms from the hippocampus[44], where the blockade of the glycogen metabolic pathway has a statistically significant impact on spatial orientation ability – positive in old mice and negative in young ones.

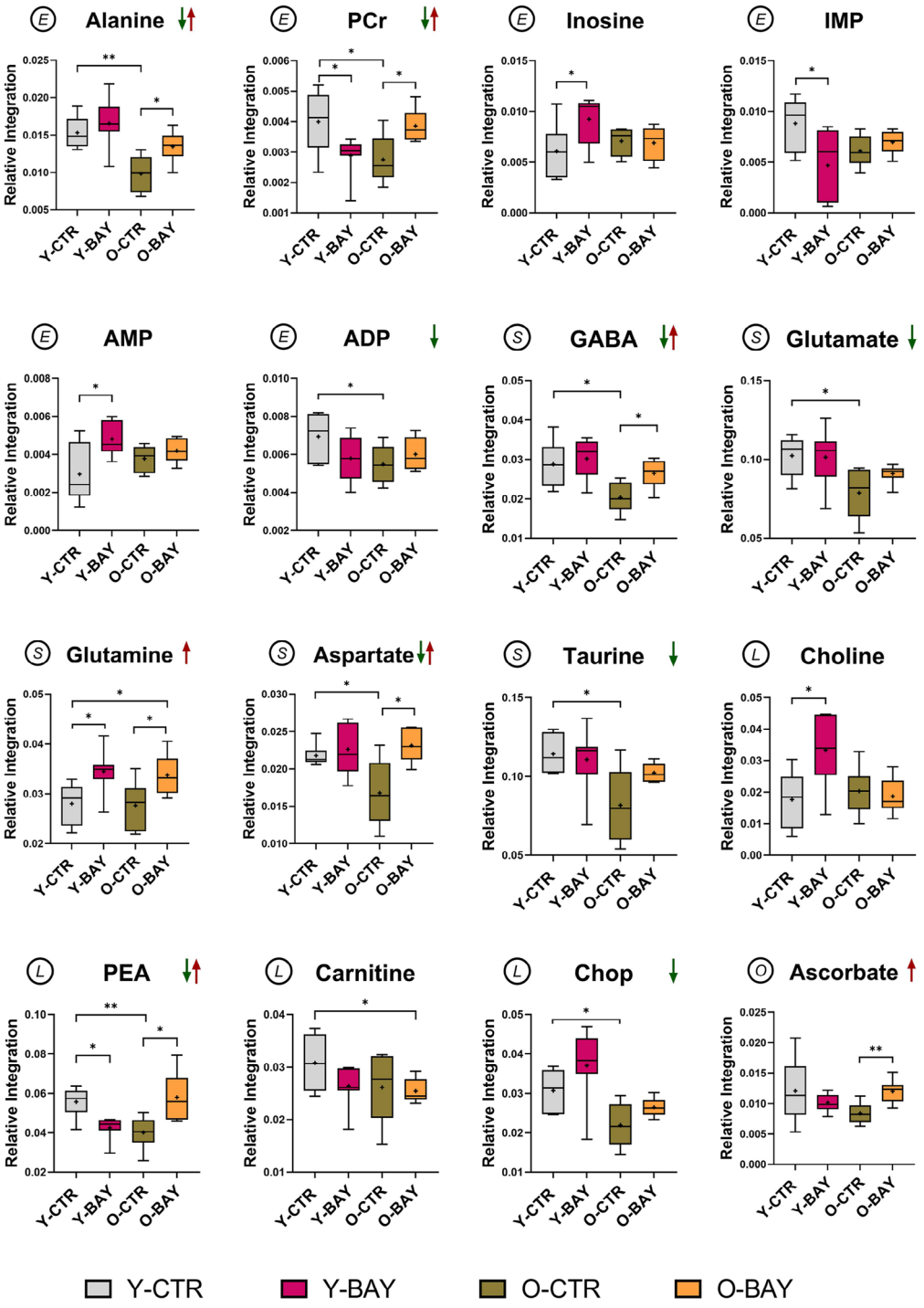

Figure 4. Box-and-whisker plots of the relative integration of significantly changed metabolites during aging and/or after BAY treatment in hippocampus. Inhibition of glycogen breakdown by a single BAY administration reversed the aging-related decrease of metabolites belonging to energy (alanine, PCr), signaling (GABA, aspartate), and lipid (PEA) pathways. Analyzed groups: young control (Y-CTR, n=6), young BAY-treated (Y-BAY, n=7), old control (O-CTR, n=6), old BAY-treated (O-BAY, n=6). The data in this figure is presented using Box and Whisker plots, where the box represents the interquartile range (IQR), showing the middle 50% of the data (from the first quartile, Q1, to the third quartile, Q3), the whiskers extend to the minimum and maximum values within the dataset, capturing the full range of the data, median value is indicated by a horizontal line within the box, providing a measure of central tendency, and mean is marked by a cross ("+") within the box, offering additional insight into the central value, particularly for normally distributed data. Statistically significant changes between groups are indicated (*$p < 0.05$; **$p < 0.01$). Green arrows indicate the age-related decrease of relative concentrations, and red arrows indicate the BAY-induced increase of relative concentrations in old animals. The letters placed in a circle assign metabolites to specific metabolic pathways: E – energy pathways, S – signaling pathways, L – lipid pathways, and O – other pathways.

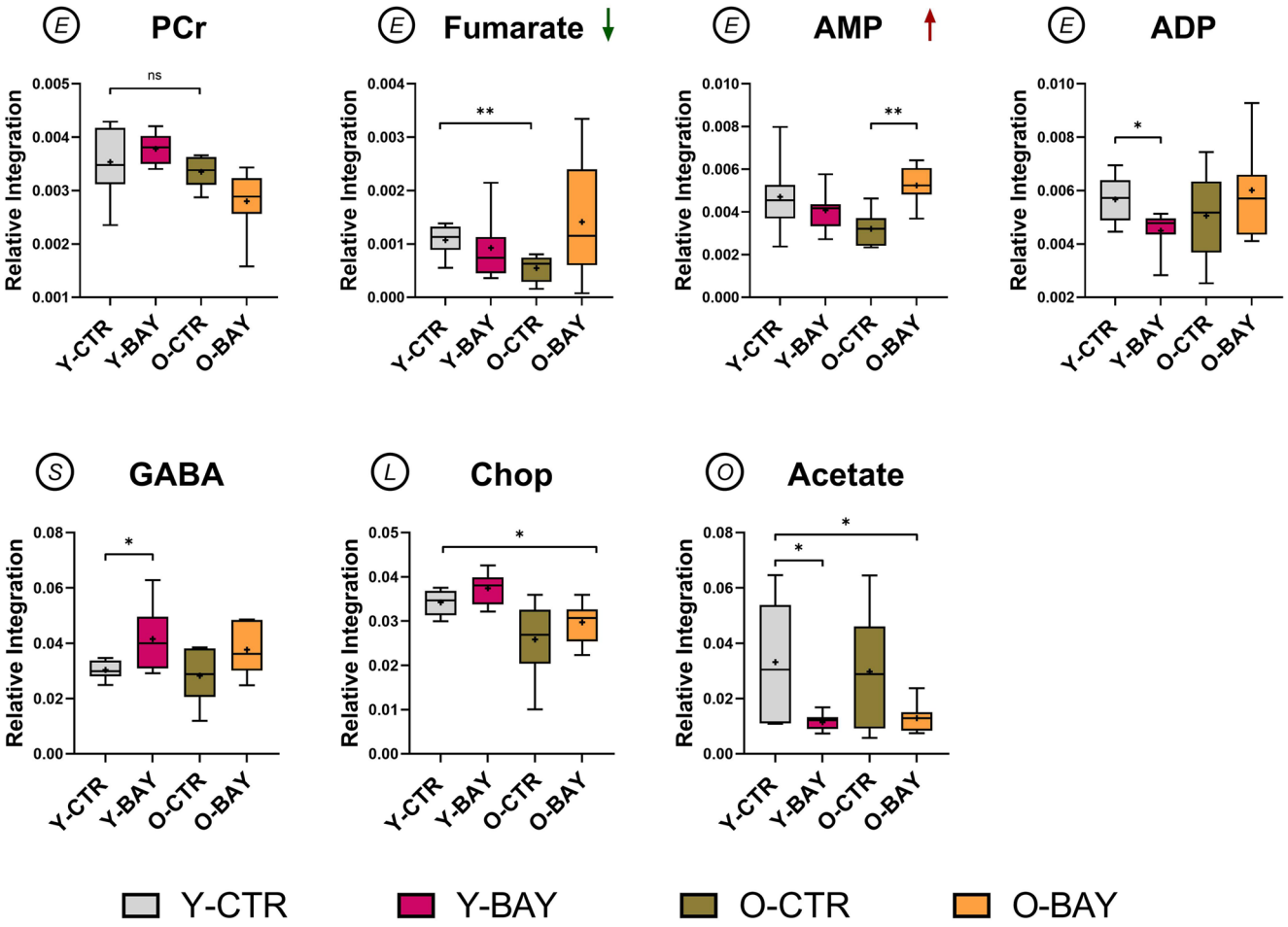

Figure 5. Box-and-whisker plots of the relative integration of significantly changed metabolites during aging and/or after BAY treatment in cortex. The cortex metabolome fingerprint underwent only a slight aging-related fluctuation, and among the 27 metabolites detected, only the fumarate titer was significantly reduced. Inhibition of glycogen breakdown with BAY significantly upregulated only AMP concentrations in old animals. Analyzed groups: young control (Y-CTR, n=8), young BAY-treated (Y-BAY, n=7), old control (O-CTR, n=6), old BAY-treated (O-BAY, n=7). The data in this figure is presented using Box and Whisker plots, where the box represents the interquartile range (IQR), showing the middle 50% of the data (from the first quartile, Q1, to the third quartile, Q3), the whiskers extend to the minimum and maximum values within the dataset, capturing the full range of the data, median value is indicated by a horizontal line within the box, providing a measure of central tendency, and mean is marked by a cross ("+") within the box, offering additional insight into the central value, particularly for normally distributed data. Statistically significant changes between groups are indicated ($^*p < 0.05$; $^{**}p < 0.01$). Green arrows indicate the age-related decrease of relative concentrations, and red arrows indicate the BAY-induced increase of relative concentrations in old animals. The letters placed in a circle assign metabolites to specific metabolic pathways: E – energy pathways, S – signaling pathways, L – lipid pathways, and O – other pathways.

Pathway view of metabolite titers in the brain affected by aging and BAY U6751 administration

The majority of alterations in metabolite levels induced by aging and BAY treatment were primarily linked to energy metabolism, particularly with the De Novo Purine Nucleotide Biosynthesis (DNPB) pathway. Furthermore, modifications within the DNPB pathway were observed across all analyzed brain regions.

(Fig. 7a, green-framed boxes). The identified metabolic shifts play a pivotal role in preserving energy homeostasis within the brain[11], thereby influencing neuronal activity, plasticity, and ultimately cognitive functions[45]. ,

Lipids represent the second-largest class of biomolecules implicated in aging, exerting, a multifaceted impact on cellular metabolism[46]. Notably, fluctuations in choline concentration, a metabolite marker for cellular membranes, have the potential to signify alterations in myelination[47]. Interestingly, it has been also shown that phosphatidylcholine (final product of Kennedy pathway) takes part in neuronal differentiation and improved neuronal alterations caused by inflammatory conditions[35,36].

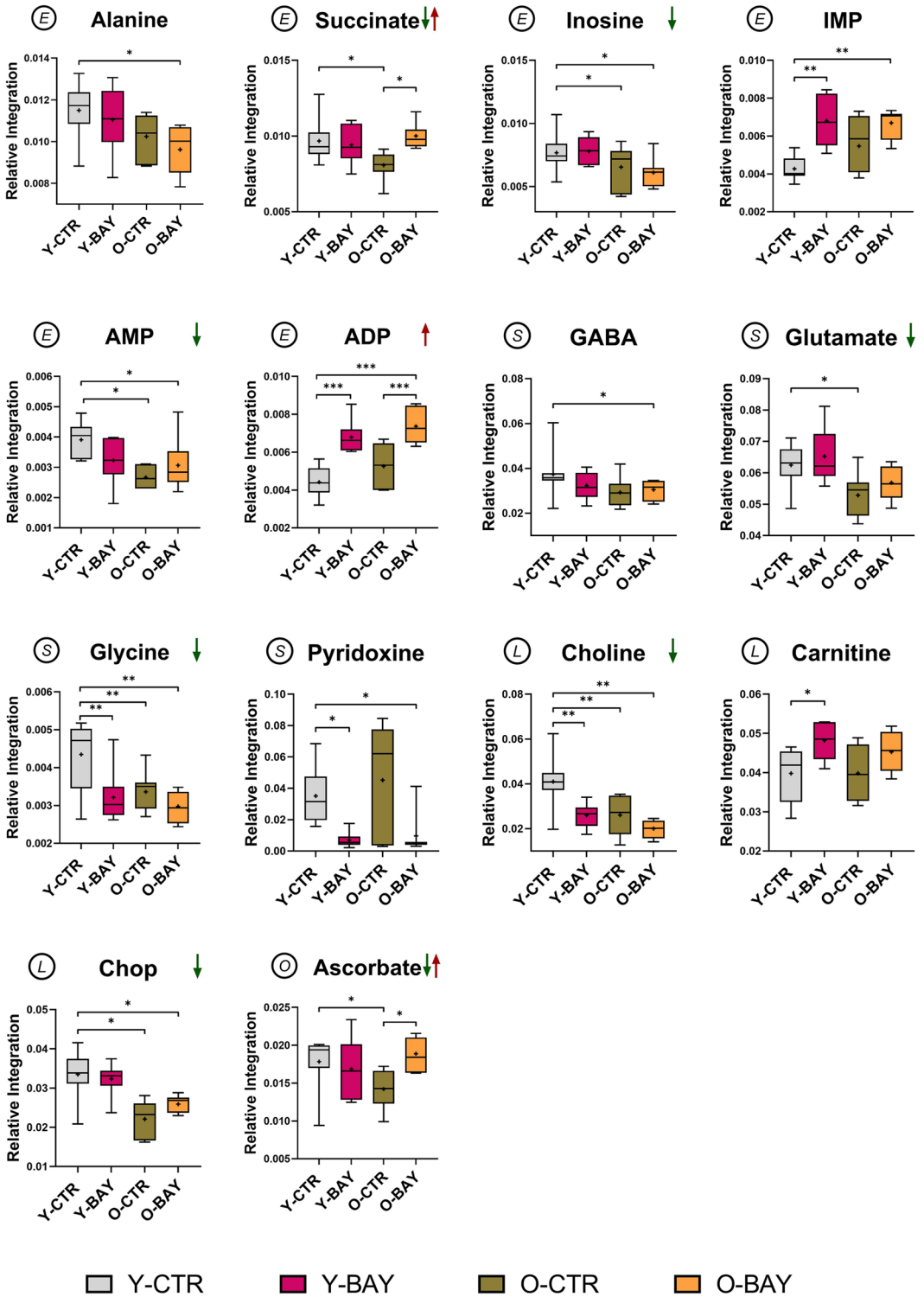
E Alanine
E Succinate
E Inosine
E IMP
E AMP
E ADP
S GABA
S Glutamate
S Glycine
S Pyridoxine
L Choline
L Carnitine
L Chop
O Ascorbate
Relative Integration
Y-CTR
Y-BAY
O-CTR
O-BAY

◀**Figure 6**. Box-and-whisker plots of the relative integration of significantly changed metabolites during aging and/or after BAY treatment in cerebellum. The cerebellum metabolome fingerprint primarily underwent aging-related reduction of metabolite titers including succinate, inosine, AMP, glutamate, glycine, choline, CHOP, ascorbate. The BAY-induced inhibition of glycogen breakdown reversed the reduction of only two metabolites (succinate and ascorbate). Analyzed groups: young control (Y-CTR, n=8), young BAY-treated (Y-BAY, n=8), old control (O-CTR, n=7), old BAY-treated (O-BAY, n=7). The data in this figure is presented using Box and Whisker plots, where the box represents the interquartile range (IQR), showing the middle 50% of the data (from the first quartile, Q1, to the third quartile, Q3), the whiskers extend to the minimum and maximum values within the dataset, capturing the full range of the data, median value is indicated by a horizontal line within the box, providing a measure of central tendency, and mean is marked by a cross ("+") within the box, offering additional insight into the central value, particularly for normally distributed data. Statistically significant changes between groups are indicated (*$p < 0.05$; **$p < 0.01$). Green arrows indicate the age-related decrease of relative concentrations, and red arrows indicate the BAY-induced increase of relative concentrations in old animals. The letters placed in a circle assign metabolites to specific metabolic pathways: E – energy pathways, S – signaling pathways, L – lipid pathways, and O – other pathways.

In our dataset, lipid metabolism exhibited notable alterations due to both aging and BAY U6751 treatment across all investigated brain regions, as depicted by the brown-framed boxes in Fig. 7a. Conversely, changes in signaling-related metabolites, including glycine, glutamine, glutamate, taurine, aspartate, and GABA, were predominantly associated with hippocampal and cerebellar formations, illustrated by the blue-framed boxes in Fig. 7a. These findings suggest that direct synaptic activity may be modulated by the inhibition of glycogen metabolism, in agreement with previous literature[2,4].

Importantly, the divergent hippocampal metabolome fingerprints in young compared to old animals (Fig. 7b), were consistent with the divergent behavioral hippocampus-dependent results of the young vs. old BAY-injected mice in the NOL test (Fig. 1e). In young animals, the decreased of IMP alongside the increased of AMP, inosine, choline and glutamine titers, were notable after BAY administration. Conversely, in old animals, these metabolites remained unchanged except glutamine, while Asp, GABA, ascorbate and alanine levels increased following BAY administration. Furthermore, the inhibition of glycogen breakdown in aged mice resulted in elevated levels of PCr in energy metabolism and PEA in lipid metabolism, contrasting the response observed in younger animals (Fig. 7b). Interestingly, we did not observe any significant changes in the relative concentration of lactate, NAD^+, or other metabolites involved in glycolysis or the TCA cycle. These results suggest that compensatory mechanisms may already normalize the energy requirements in the hippocampus. Recent reports propose that glycogen-derived lactate should not solely be regarded as a byproduct of anaerobic metabolism but may also serve as a signaling molecule[48]. Furthermore, our previous data indicate that the time-specific extracellular administration of lactate is essential for the induction of long-term potentiation efficacy[49,50].

Although the significance of astrocyte glycogen-derived lactate and consequently, glycogen metabolism for memory formation has been extensively documented[3,51–53], the molecular mechanism of this phenomenon is not fully understood. It has been hypothesized that astrocytes and neurons form a tripartite synapse[54], and during the LTP formation, astrocytic glycogen-derived lactate is taken up by neurons (presumably by the pre- and/or postsynaptic parts of neuronal contacts) and oxidized to pyruvate, which is coupled with an increase locally in the NADH/NAD^+ ratiowithin synaptic connections. Moreover, the increased ratio potentiates signaling via NMDA receptors[55], and promotes Camk2 autoactivation by dimeric fructose 1,6-bisphosphatase 2 (Fbp2)[50], an enzyme whose oligomerization (tetramerization) is NAD^+- and AMP-dependent[49].

The outlined mechanisms suggest a signaling role for lactate derived from astrocytic glycogen, rather than its involvement in increasing the metabolic rate. This notion aligns with data demonstrating that the levels of glycogen and glycogen metabolism enzymes in the brain are relatively low compared to other cells and organs that store glycogen[56]. Therefore, it seems unlikely that the release of glucosyl units from glycogen can substantially modulate the levels of glycolytic metabolites throughout the entire brain or specific formations, thus impacting their overall metabolic activity.

Conclusion

In this study, we have demonstrated that the administration of a single dose of BAY U6751 (BAY) elicited effects on cognitive performance lasting for at least 5 h, as assessed by the Novel Object Location test. Moreover, this single dose of BAY also significantly impacted the metabolic status of all brain regions studied, with particularly pronounced effects observed in the hippocampal and cerebellar formations. These findings not only deepen our understanding of age-related alterations in brain metabolism but also highlight the intricate relationship between glycogenolysis and neuroplasticity. Further exploration in this direction holds promise for addressing age-related cognitive decline and neurodegenerative processes.

The prolonged and widespread impact of Pyg inhibition suggests lactate as a factor modulating the activity of signaling proteins involved in the expression of genes encoding enzymes across several distinct metabolic pathways. Although the precise mechanism through which lactate influences such expression remains unknown[2], the positive influence of BAY on memory formation in aged animals suggests that this avenue warrants further investigation as a promising target for anti-aging therapy.

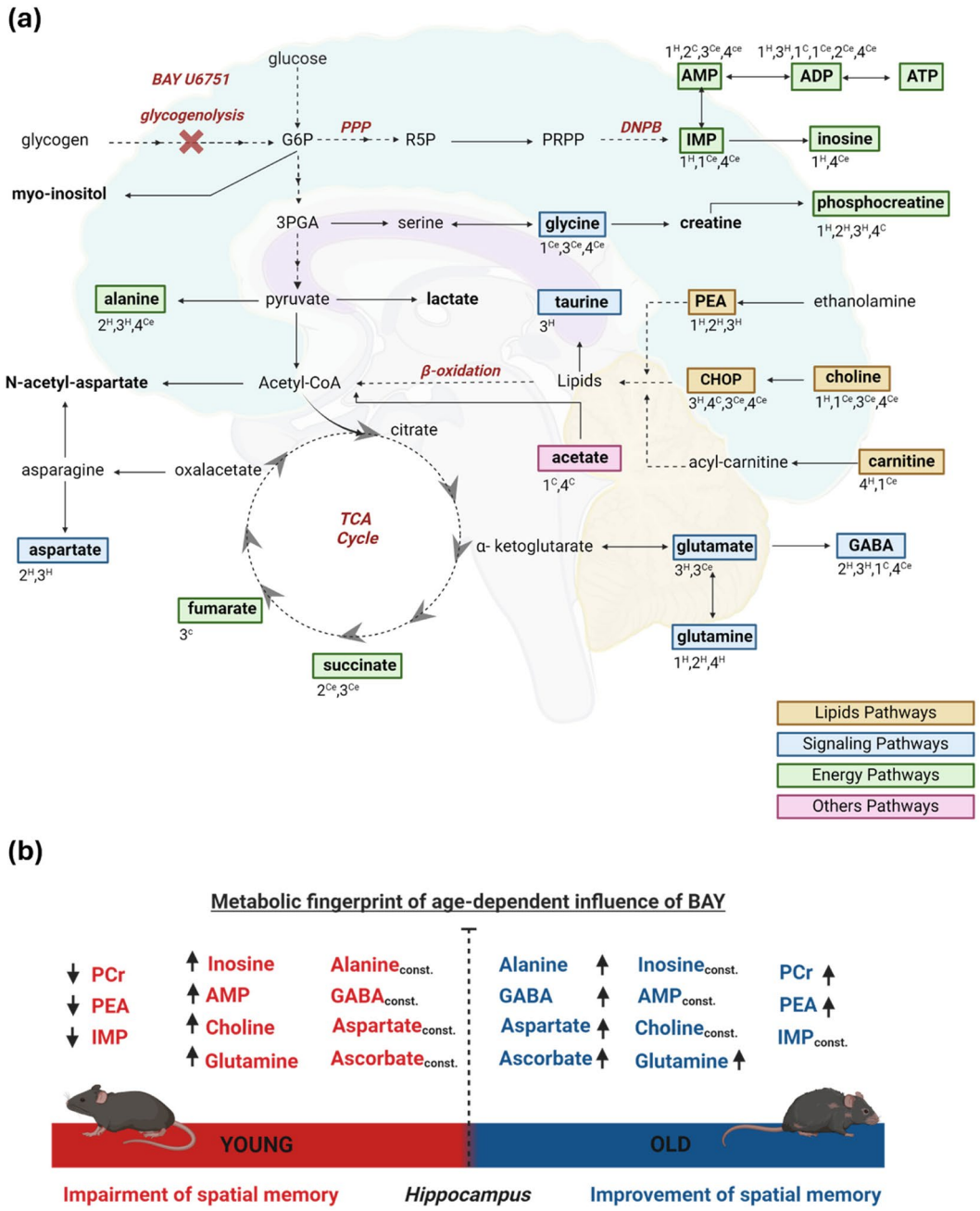

Figure 7. Schematic overview of age-dependent BAY-induced changes in metabolite levels. (**a**) Crosstalk of metabolic pathways linked to altered levels of identified metabolites. Detected metabolites are bolded. Metabolites showing statistically significant changes with aging or after BAY-treatment are classified into three general pathways: energy pathways (green-framed boxes), signaling pathways (blue-framed boxes), lipid pathways (brown-framed boxes), and others (pink-framed boxes). Additionally, these metabolites are assigned to brain structures in which they titers changed in: 1 – Y-CTR vs. Y-BAY, 2 – O-CTR vs. O-BAY, 3- Y-CTR vs. O-CTR, and 4 – Y-CTR vs. O-BAY; H – hippocampus, C – cortex, Ce – cerebellum (for example: 1^{H} means that a given metabolite changes significantly in Y-CTR in comparison to Y-BAY in the hippocampus). The remaining abbreviations: Chop – O-phosphocholine, DNPB – De Novo Purine Nucleotide Biosynthesis Pathway, G6P – Glucose-6-phosphate, PPP – Pentose Phosphate Pathway, PRPP – 5-phosphoribosyl-1-pyrophosphate, R5P – Ribose-5-phosphate, 3PGA – 3-Phosphoglyceric acid, PEA – O-phosphoethanolamine. The red "x" indicates the blockade of glycogenolysis by BAY U6751. Metabolites of various pathways origins (NAD+, pyridoxine, and ascorbate) are not included in the scheme. (**b**) The metabolomic fingerprint of age-dependent influence of BAY on young and old animals, in the context of changes of spatial memory formation in hippocampus. Const. indicates lack of changes; arrows mark an increase or decrease in metabolite titers.

Materials and methods

Materials

All needed basic chemicals (methanol, chloroform, HPLC deionized water) were purchased from Merck KGaA (Darmstadt, Germany). The deuterium oxide (99.9% D), MagniSolv™ for NMR spectroscopy, sodium phosphate dibasic (Na_2HPO_4), sodium phosphate monobasic (NaH_2PO_4), sodium azide (NaN_3), and 3-(Trimethylsilyl) propionic-2,2,3,3-d_4 acid sodium salt (TSP) were purchased from Sigma-Aldrich (Darmstadt, Germany). BAY U6751 (BAY) glycogen phosphorylase inhibitor was purchased from Santa Cruz Biotechnology (Dallas, Texas, USA). 5 mm NMR tubes, type 5SP from Armar Chemicals (Germany) were utilized.

Animals

Male C57BL/6J mice, 2-month-old (further referred to as young [Y]; $n=15$), and 20-22-month-old mice (further referred to as old [O]; $n=20$), were obtained from Nencki Institute of Experimental Biology PAS, Warsaw, Poland, and housed in pairs under the 12 h/12 h light/dark cycle, with food and water available *ad libitum*. Each age group was further subdivided into four experimental groups: saline solution injection (Y-CTR, $n=7$, and O-CTR, $n=10$), and BAY injection (Y-BAY, $n=8$, and O-BAY, $n=10$).

All experiments were carried out in accordance with the Polish guidelines and regulations regarding the care and the use of animals for experimental procedures and approved by the Wroclaw Ethical Committee (permission no. 041/2023). All efforts were made to minimize the number of animals used in the experiments and to limit their distress and suffering.

Behavioral tests

To assess whether a single intraperitoneal injection of glycogen phosphorylase inhibitor (BAY) could influence memory formation, all animals underwent testing in two rounds of well-established behavioral tasks commonly employed to elucidate the role of specific brain regions in memory processes: the 2-Novel Object Recognition (NOR) and the Novel Object Location test (NOL), hereinafter referred to as NOL + NOR test, separated by a pharmacological intervention.

Before testing, mice underwent a handling procedure for 5 min each day over 7 days. This handling protocol was implemented to mitigate potential stress or anxiety in the animals.

The first round of the NOL + NOR was performed in Day 0 in order to establish the animal's baseline cognitive skills (young mice were 8-weeks-old at the time of this test, old mice were 20–22-months-old). Following this, a one-week break was implemented, and a single intraperitoneal injection of the glycogen phosphorylase inhibitor BAY U6751 (25 µg per 1 g of tissues, in 0.9% NaCl) or a 0.9% saline solution was administered. The final concentration in the injected dose was standardized to 5 µM.

The working concentration of BAY injections was determined through ex vivo and in vivo studies and is detailed in our prior publication (see Supplementary Materials[2]). Moreover, the determined effective BAY concentration in mouse tissues 6 h after intraperitoneal administration[57] is sufficient to block the Pyg activity according to enzyme-inhibitor kinetic parameters[58]. The potential impact of BAY on locomotor skills, glucose concentration in the blood, or body mass was systematically monitored and is discussed in the cited publication[2].

Four and a half hours after the injection, the NOL + NOR test was repeated. The NOL + NOR test we performed in the dark phase maintained the time of the circadian cycle of mice and their order in the tests for Day 0 and at day "One Dose of BAY". Finally, six hours post-injection, the animals were anesthetized using 2% isoflurane compound, and sacrificed by decapitation. The whole brain was dissected into 3 different brain structures (hippocampus, cortex, and cerebellum), and immediately snap-frozen in liquid nitrogen and stored at -80°C until preparation for NMR data acquisition.

Novel object location (NOL) and 2-Novel object Recognition (NOR) test – NOL + NOR test

The NOL and NOR test was conducted following the methodology outlined by Denninger, Smith, and Kirby[23]. Testing was conducted in an open field arena constructed from white opaque material with dimensions of 33 cm × 33 cm × 20 cm (length, width, height, respectively) and with top lightning (5 lx intensity). 24 h before testing (Day 0), each mouse was habituated (10 min) to the empty box. The NOL + NOR test consisted of the familiarization session (10 min), when the mouse was allowed to explore two identical objects in the box; the intersession interval (30 min); the NOL test session (10 min), when the mouse was returned to the box, where one of the familiar objects changed location; the second intersession interval (30 min); the NOR test session (10 min), when the mouse was returned to the box, with one familiar and one novel object (the novel object was different in shape, texture and color). To eliminate any residual scent, both the test box and objects were cleaned with ethanol and water after each session. Additionally, to minimize stress and anxiety associated with the removal of a single animal from the cage, which could potentially reduce the animal's motivation to explore the arena and objects, each pair of animals from the same cage was simultaneously tested in identical boxes with an identical set of objects.

The behavior of mice during the sessions was recorded by a digital camera positioned approximately 1.5 m above the box. After the single injection of BAY, the NOL + NOR test was repeated with novel objects. A graphical representation of the test design is shown in Fig. 1a.

NOL + NOR behavioral analyses

To ascertain results for the NOR and NOL tests, video recordings were meticulously analyzed using a self-developed analysis system.

The exploration time was defined as the duration during which the distance of the mouse's nose to an object was no more than 2 cm, facing toward the object. In instances where mice climbed onto the object using all four

paws, the exploration time was not computed. The analysis proceeded until the criterion of a cumulative 20 seconds of exploration (combined for both objects) was achieved.

The amount of time the mouse spent exploring the object 1 vs. object 2 (in the familiarization session), constant vs. moved object (in the NOL session), and familiar vs. novel object (in the NOR session) were used to measure, respectively, the site preference, the hippocampus-dependent (spatial memory) and mainly cortex-dependent (object recognition) cognitive skills[22,23].

Samples preparation and NMR measurements

The frozen brain tissue (hippocampus, cortex, or cerebellum) was broken apart in a liquid N_2-cooled pestle and mortal. Then it was carefully weighted into an Eppendorf tube for a final mass of ~ 30 mg. It is important to note that samples remained frozen throughout the preparation. The extraction of polar metabolites followed a multistep procedure utilizing ice-cold solvents, namely methanol, chloroform, and water. In the initial step, 380 µL of methanol was added, and the mixture was homogenized at a frequency of 25 Hz using TissueLyser LT (QIAGEN, Germantown, USA) for 5 min. Subsequently, 190 µL of chloroform and 190 µL of water were added, followed by homogenization at a 25 Hz oscillation frequency for an additional 5 min. The resulting samples were then centrifuged (Micro 220R, Hettich) at 10,000 rpm for 15 min at 4 °C. The supernatant was carefully transferred to a new Eppendorf tube and subjected to evaporation using a vacuum centrifuge (WP-03, JW Electronic, United States) at 1500 rpm for 6 h at 45 °C.

Polar tissue extracts were reconstituted in 580 µL of NMR buffer (0.5 M sodium phosphate buffer, pH 7.4, in 10% D_2O containing 1 mM TSP and 1 g NaN_3). Subsequently, 550 µL of the reconstituted solution was drawn and transferred to 5 mm NMR tubes. After that, the samples were stored at 4 °C before acquiring the ^{1}H NMR spectra, which were obtained immediately after sample preparation.

^{1}H NMR spectroscopy analysis

The one-dimensional (1D) NMR spectra of the brain tissue extract were acquired utilizing the 1D NOESY water suppression pulse sequences (on noesypr1d, Bruker notation) at 300 K, employing an Avance II spectrometer (Bruker, GmBH, Germany) with a proton frequency of 600.58 MHz. The sequential parameters employed were as follows: relaxation delay (RD) of 4.0 s, acquisition time of 1.36 s, total number of scans set to 128, mixing time of 125 ms, time domain data points at 32.768, and receiver gain at 36. Subsequently, the acquired spectra underwent processing with a line broadening of 0.3 Hz and manual phasing using Topspin 1.3 software (Bruker, GmBH, Germany). Baseline correction was executed using the Whittaker smoother algorithm in MestReNova software (MestReNova v. 14.2.3, Qingdao, China), and referenced to the TSP resonance at 0.0 ppm.

Univariate processing and statistical data analysis

All acquired spectra were imported into MATLAB (Matlab R2014a, v. 8.3.0.532, Natick, MA, USA) for preprocessing. The spectral regions corresponding to the cortex and cerebellum, spanning from 4.53 to 5.64 ppm, and for the hippocampus, ranging from 4.52 to 5.79 ppm, were excluded from the data analysis to eliminate water resonance signals. Resonance signal alignment procedures were executed using the correlation optimized wrapping (COW)[59] and interval correlation shifting (icoshift)[60] algorithms. The spectra, consisting of 8910 data points, were then normalized utilizing the probabilistic quotient normalization (PQN)[61] method.

Identification of metabolites was performed using Chenomx software (v 8.5 Chenomx Inc. Edmonton, Alberta, Canada), along with verification from the Human Metabolome Database24 (www.hmdb.ca) and relevant literature. For statistical analysis, a single signal for each metabolite was employed, and the representative signals with NMR assignments are presented in the supplementary materials (Table S1) excluding ATP – the identified metabolite which lacked a discernible resonance signal of its own. Univariate analysis was carried out using MATLAB software. Depending on the distribution of the data, Student's t-test (equal/unequal variance) was employed for a nominal distribution, and the Mann-Whitney-Wilcoxon test was applied for a non-parametric distribution. The normality of the distribution was assessed using the Shapiro–Wilk test. All univariate statistics were performed at a significance level of p-value < 0.05. The relative integration values, expressed as means or medians depending on the statistical distribution, are presented in the Supplementary data (Table S3-S5). The multivariate analysis was performed on a set of the assigned metabolites. The relative integration (relative concentration) of metabolites measured by NMR was obtained as the sum of data points in the data matrix for the non-overlapping resonances. Next, the *prcomp()* function in the R programming language was applied to the selected matrix dataset to perform the Principal Component Analysis (PCA) by using singular value decomposition (SVD) of the centered and scaled data matrix. To visualize the PCA-biplots results in plots showing individual observation, variable contributions, and overall dataset structure, we applied *factoextra::fviz_pca_biplot* function in the R programming language.

Data availability

The datasets used and/or analysed during the current study available from the corresponding author on reasonable request.

Received: 24 May 2024; Accepted: 30 September 2024
Published online: 15 October 2024

References

1. Gibbs, M. E., O'dowd, B. S., Hertz, E. & Hertz, L. Astrocytic energy metabolism consolidates memory in young chicks. *Neuroscience*. **141**, 9–13 (2006).
2. Drulis-Fajdasz, D. et al. Glycogen phosphorylase inhibition improves cognitive function of aged mice. *Aging Cell*.**22**, 1–18. https://doi.org/10.1111/acel.13928 (2023).

3. Suzuki, A. et al. Astrocyte-neuron lactate transport is required for long-term memory formation. *Cell*. **144**, 810–823 (2011).
4. Drulis-Fajdasz, D. et al. Involvement of cellular metabolism in age-related LTP modifications in rat hippocampal slices. *Oncotarget*. **6**, 14065–14081 (2015).
5. Magistretti, P. J. & Allaman, I. A Cellular Perspective on Brain Energy Metabolism and Functional Imaging. *Neuron*. **86**, 883–901 (2015).
6. Drulis-Fajdasz, D., Gizak, A., Wójtowicz, T., Wiśniewski, J. R. & Rakus, D. Aging-associated changes in hippocampal glycogen metabolism in mice. Evidence for and against astrocyte-to-neuron lactate shuttle. *Glia*. **66**, 1481–1495 (2018).
7. Drulis-Fajdasz, D., Gostomska-Pampuch, K., Duda, P., Wiśniewski, J. R. & Rakus, D. Quantitative proteomics reveals significant differences between mouse brain formations in expression of proteins involved in neuronal plasticity during aging. *Cells.* **10**, 1-26 (2021).
8. Zhu, X. H., Lu, M., Lee, B. Y., Ugurbil, K. & Chen, W. In vivo NAD assay reveals the intracellular NAD contents and redox state in healthy human brain and their age dependences. *Proc. Natl. Acad. Sci. U S A*. **112**, 2876–2881 (2015).
9. Fang, W. et al. Metabolomics in aging research: aging markers from organs. *Front. Cell. Dev. Biol.***11**, 1–21 (2023).
10. Ryan, D., Robards, K. & Metabolomics The greatest omics of them all? *Anal. Chem.***78**, 7954–7958 (2006).
11. Ivanisevic, J. et al. Metabolic drift in the aging brain. *Aging (Albany NY)*. **8**, 1000–1020 (2016).
12. Abreu, A. C., Navas, M. M., Fernandez, C. P., Sanchez-Santed, F. & Fernandez, I. NMR-Based Metabolomics Approach to explore Brain Metabolic Changes Induced by prenatal exposure to Autism-Inducing Chemicals. *ACS Chem. Biol.***16**, 753–765 (2021).
13. Gonzalez-Riano, C., Garcia, A. & Barbas, C. Metabolomics studies in brain tissue: a review. *J. Pharm. Biomed. Anal.***130**, 141–168 (2016).
14. Akimoto, H. et al. Changes in brain metabolites related to stress resilience: metabolomic analysis of the hippocampus in a rat model of depression. *Behav. Brain Res.***359**, 342–352 (2019).
15. Zheng, H. et al. Analysis of neuron-astrocyte metabolic cooperation in the brain of db/db mice with cognitive decline using 13 C NMR spectroscopy. *J. Cereb. Blood Flow. Metab.***37**, 332–343 (2017).
16. Crook, A. A. & Powers, R. Quantitative NMR-Based Biomedical Metabolomics: current status and applications. *Molecules.* **25**, 1-33 (2020).
17. Beckonert, O. et al. Metabolic profiling, metabolomic and metabonomic procedures for NMR spectroscopy of urine, plasma, serum and tissue extracts. *Nat. Protoc.***2**, 2692–2703 (2007).
18. Warburton, E. C. & Brown, M. W. Findings from animals concerning when interactions between perirhinal cortex, hippocampus and medial prefrontal cortex are necessary for recognition memory. *Neuropsychologia*. **48**, 2262–2272 (2010).
19. Bannerman, D. M. et al. Hippocampal synaptic plasticity, spatial memory and anxiety. *Nat. Rev. Neurosci.***15**, 181–192 (2014).
20. Harris, M. A., Wiener, J. M. & Wolbers, T. Aging specifically impairs switching to an allocentric navigational strategy. *Front. Aging Neurosci.***4**, 1–9 (2012).
21. Grayson, B. et al. Assessment of disease-related cognitive impairments using the novel object recognition (NOR) task in rodents. *Behav. Brain Res.***285**, 176–193 (2015).
22. Antunes, M. & Biala, G. The novel object recognition memory: Neurobiology, test procedure, and its modifications. *Cogn. Process.***13**, 93–110 (2012).
23. Denninger, J. K., Smith, B. M. & Kirby, E. D. Novel object recognition and object location behavioral testing in mice on a budget. *J. Vis. Exp.***20**, 1–10 (2018).
24. Chhetri, D. R. Myo-Inositol and its derivatives: their emerging role in the treatment of human diseases. *Front. Pharmacol.***10**, 1–8 (2019).
25. Castro, M. A., Beltrán, F. A., Brauchi, S. & Concha I. I. A metabolic switch in brain: glucose and lactate metabolism modulation by ascorbic acid. *J. Neurochem.* **110**, 423–440 (2009).
26. Waniewski, R. A. & Martin, D. L. Preferential utilization of acetate by astrocytes is attributable to transport. *J. Neurosci.***18**, 5225–5233 (1998).
27. Manto, M. et al. Consensus paper: roles of the cerebellum in motor control-the diversity of ideas on cerebellar involvement in movement. *Cerebellum*. **11**, 457–487 (2012).
28. Bird, C. M. & Burgess, N. The hippocampus and memory: insights from spatial processing. *Nat. Rev. Neurosci.***9**, 182–194 (2008).
29. Rozycka, A. et al. Glutamate, GABA, and presynaptic markers involved in neurotransmission are differently affected by age in distinct mouse brain regions. *ACS Chem. Neurosci.***10**, 4449–4461 (2019).
30. Rozycka, A. & Liguz-Lecznar, M. The space where aging acts: focus on the GABAergic synapse. *Aging Cell.***16**, 634–643 (2017).
31. Fontana, A. C. K. current approaches to enhance glutamate transporter function and expression. *J. Neurochem.* **134**, 982–1007 (2015).
32. Waagepetersen, H. S., Sonnewald, U., Larsson, O. M. & Schousboe, A. A possible role of alanine for ammonia transfer between astrocytes and glutamatergic neurons. *J. Neurochem*. **75**, 471–479 (2000).
33. Dadsetan, S. et al. Brain alanine formation as an ammonia-scavenging pathway during hyperammonemia: effects of glutamine synthetase inhibition in rats and astrocyte-neuron co-cultures. *J. Cereb. Blood Flow. Metab.***33**, 1235–1241 (2013).
34. Schousboe, A., Sonnewald, U. & Waagepetersen, H. S. Differential roles of alanine in GABAergic and glutamatergic neurons. *Neurochem Int.***43**, 311–315 (2003).
35. Marcucci, H., Paoletti, L., Jackowski, S. & Banchio, C. Phosphatidylcholine biosynthesis during neuronal differentiation and its role in cell fate determination. *J. Biol. Chem.***285**, 25382–25393 (2010).
36. Magaquian, D., Delgado Ocaña, S., Perez, C. & Banchio, C. Phosphatidylcholine restores neuronal plasticity of neural stem cells under inflammatory stress. *Sci. Rep.***11**, 1–12 (2021).
37. Ellison, D. W., Beal, M. F. & Martin, J. B. Phosphoethanolamine and ethanolamine are decreased in Alzheimer's disease and Huntington's disease. *Brain Res.***417**, 389–392 (1987).
38. Klunk, W. E., Debnath, M. L., McClure, R. J. & Pettegrew, J. W. Inactivity of phosphoethanolamine, an endogenous GABA analog decreased in Alzheimer's disease, at GABA binding sites. *Life Sci.***56**, 2377–2383 (1995).
39. Blusztajn, J. K. & Slack, B. E. Accelerated breakdown of Phosphatidylcholine and Phosphatidylethanolamine is a predominant brain metabolic defect in Alzheimer's Disease. *J. Alzheimer's Dis.***93**, 1285–1289 (2023).
40. Carter, A. J., Müller, R. E., Pschorn, U. & Stransky, W. Preincubation with Creatine Enhances Levels of Creatine Phosphate and prevents anoxic damage in rat hippocampal slices. *J. Neurochem*. **64**, 2691–2699 (1995).
41. Jost, C. R. et al. Creatine kinase B-driven energy transfer in the brain is important for habituation and spatial learning behaviour, mossy fibre field size and determination of seizure susceptibility. *Eur. J. Neurosci.***15**, 1692–1706 (2002).
42. Majkutewicz, I. et al. Age-dependent effects of dimethyl fumarate on cognitive and neuropathological features in the streptozotocin-induced rat model of Alzheimer's disease. *Brain Res.***1686**, 19–33 (2018).
43. Popesco, M. C. et al. Serial analysis of gene expression profiles of adult and aged mouse cerebellum. *Neurobiol. Aging*. **29**, 774–788 (2008).
44. Woodruff-Pak, D. et al. Differential effects and rates of normal aging in cerebellum and hippocampus. *Proc. Natl. Acad. Sci. U. S. A.***107**, 1624–1629 (2010).
45. Kaiser, L. G., Schuff, N., Cashdollar, N. & Weiner, M. W. Age-related glutamate and glutamine concentration changes in normal human brain: 1H MR spectroscopy study at 4 T. *Neurobiol. Aging*. **26**, 665–672 (2005).
46. Lu, Y. et al. Multi-omics analysis reveals neuroinflammation, activated glial signaling, and dysregulated synaptic signaling and metabolism in the hippocampus of aged mice. *Front. Aging Neurosci.***14**, 1–18 (2022).

47. Gudi, V., Grieb, P., Linker, R. A. & Skripuletz, T. CDP-choline to promote remyelination in multiple sclerosis: the need for a clinical trial. *Neural Regen Res.***18**, 2599–2605 (2023).
48. Magistretti, P. J. & Allaman, I. Lactate in the brain: from metabolic end-product to signalling molecule. *Nat. Rev. Neurosci.***19**, 235–249 (2018).
49. Gizak, A., Duda, P., Wisniewski, J. & Rakus, D. Fructose-1,6-bisphosphatase: from a glucose metabolism enzyme to multifaceted regulator of a cell fate. *Adv. Biol. Regul.***72**, 41–50 (2019).
50. Duda, P. et al. Fructose 1,6-Bisphosphatase 2 plays a crucial role in the induction and maintenance of long-term potentiation. *Cells.* **9**, 1–22 (2020).
51. Duran, J., Saez, I., Gruart, A., Guinovart, J. J. & Delgado-García, J. M. Impairment in long-term memory formation and learning-dependent synaptic plasticity in mice lacking glycogen synthase in the brain. *J. Cereb. Blood Flow. Metab.***33**, 550–556 (2013).
52. Brown, A. M. Brain glycogen re-awakened. *J. Neurochem.* **89**, 537–552 (2004).
53. Bak, L. K. & Walls, A. B. Astrocytic glycogen metabolism in the healthy and diseased brain. *J. Biol. Chem.***293**, 7108–7116 (2018).
54. Haydon, P. G. & Glia Listening and talking to the synapse. *Nat. Rev. Neurosci.***2**, 185–193 (2001).
55. Yang, J. et al. Lactate promotes plasticity gene expression by potentiating NMDA signaling in neurons. *Proc. Natl. Acad. Sci. U S A.* **111**, 12228–12233 (2014).
56. Wu, L., Butler, N. J. M. & Swanson, R. A. Technical and comparative aspects of brain glycogen metabolism. *Adv. Neurobiol.***23**, 169–185 (2019).
57. Pudelko-Malik, N., Wiśniewski, J., Drulis-Fajdasz, D. & Mlynarz, P. Validated liquid chromatography-mass spectrometry method for the quantification of glycogenolysis phosphorylase inhibitor in mouse tissues – 5-isopropyl-4-(2-chlorophenyl)-1-ethyl-1,4-dihydro-6-methyl-2,3,5-pyridinetricarboxylic acid ester disodium salt hydrate. *J. Sep. Sci.***45**, 3791–3799 (2022).
58. Bergans, N., Stalmans, W., Goldmann, S. & Vanstapel, F. Molecular mode of inhibition of glycogenolysis in rat liver by the dihydropyridine derivative, BAY R3401: inhibition and inactivition of glycogen phosphorylase by an activated metabolite. *Diabetes*. **49**, 1419–1426 (2000).
59. Tomasi, G., Van Den Berg, F. & Andersson, C. Correlation optimized warping and dynamic time warping as preprocessing methods for chromatographic data. *J. Chemom.* **18**, 231–241 (2004).
60. Savorani, F., Tomasi, G. & Engelsen, S. B. Icoshift: a versatile tool for the rapid alignment of 1D NMR spectra. *J. Magn. Reson.***202**, 190–202 (2010).
61. Dieterle, F., Ross, A. & Senn, H. Probabilistic quotient normalization as robust method to aacount for dilution of complex biuological mixtures. *Anal. chem.***78**, 4281–4290 (2006).

Author contributions

N.P.-M., D. D.-F., D. R., A. G. and P. M. wrote the main manuscript. N. P.-M., D. D.-F., and K. A. M.-N. prepared the methodology. N.P.-M. and D. D.-F. prepared the investigation. N.P.-M., D. D.-F. and Ł. P. prepared the data visualization. D. D.-F., D. R., A. G. and P.M. prepared the conceptualization and review of the article. D. R. and P. M. supervised the studies. All authors reviewed the manuscript.

Funding

This research was funded by the Polish National Science Centre: UMO-2020/37/B/NZ4/00808.

Declarations

Ethical approval

All experiments were carried out in accordance with the Polish guidelines and regulations regarding the care and the use of animals for experimental procedures and approved by the Wroclaw Ethical Committee (permission no. 041/2023). All efforts were made to minimize the number of animals used in the experiments and to limit their distress and suffering. All experiments were performed in accordance with ARRIVE guidelines.

Competing interests

The authors declare no competing interests.

Additional information

Supplementary Information The online version contains supplementary material available at https://doi.org/10.1038/s41598-024-74861-z.

Correspondence and requests for materials should be addressed to A.G. or P.M.